

The Role of Cuprous Oxide Seeds in the One-Pot and Seeded Syntheses of Copper Nanowires

Shengrong Ye, Aaron R. Rathmell, Yoon-Cheol Ha, Adria R. Wilson, and Benjamin J. Wiley*

This paper demonstrates that Cu_2O nanoparticles form in the early stages of a solution-phase synthesis of copper nanowires, and aggregate to form the seeds from which copper nanowires grow. Removal of ethylenediamine from the synthesis leads to the rapid formation of Cu_2O octahedra. These octahedra are introduced as seeds in the same copper nanowire synthesis to improve the yield of copper nanowires from 12% to >55%, and to enable independent control over the length of the nanowires. Transparent conducting films are made from nanowires with different lengths to examine the effect of nanowire aspect ratio on the film performance.

1. Introduction

This paper reveals the role of cuprous oxide (Cu_2O) in the synthesis of copper nanowires, and introduces the first seeded synthesis to produce copper nanowires with controlled dimensions. Cu_2O seeds form in the early stages of a one-pot copper nanowire synthesis, and are the precursors to the copper seeds from which copper nanowires grow.^[1] In the absence of ethylenediamine (EDA), these Cu_2O seeds grow to form Cu_2O octahedra in a matter of minutes, consuming the ionic copper precursor. This result suggests that EDA suppresses the precipitation of Cu_2O , and keeps the ionic copper precursor in a form from which it can be converted to nanowires. Using this new mechanistic information, we synthesized Cu_2O octahedra separately and added them as seeds to a copper nanowire synthesis. The addition of seeds enabled control over the length of copper nanowires, and

improved the reaction yield from 12% to >55%. We used batches of copper nanowires of the same width but different lengths to examine the effect of nanowire length on the properties of transparent conducting films. This study shows that a seeded approach to nanowire synthesis can improve control over the dimensions of metal nanowires, and thereby serve to clarify the relationship between the structure and properties of metal nanowires.

Metal nanowires have potential uses in a variety of applications,^[2] including as a supplement or replacement of indium tin oxide (ITO) as a transparent conductor in touch screens, OLEDs, and organic solar cells.^[3] Solution-phase synthesis is the preferred method of nanowire production for transparent conducting films due to its relative scalability and low-cost.^[1] It is important to precisely control the dimensions of the metal nanowires grown in solution for consistent commercial production, as well as to better understand how the dimensions of nanowires affect their properties in various applications. However, in most nanowire syntheses used today, it is challenging to independently control the length and diameter of nanowires. For example, changing synthesis conditions to increase nanowire length usually increases their diameter as well.^[4]

Progress on dimensional control of Ag and Au nanowires (NWs) has been made through the use of seed-mediated syntheses.^[5] Murphy and coworkers demonstrated Ag NWs with controllable aspect ratios (50–350) could be produced using Ag nanoparticles as seeds.^[5a] Lee *et al.* developed a successive multistep growth method to increase the length of Ag NWs up to 500 μm while maintaining the average

Dr. S. Ye, Dr. A. R. Rathmell,
A. R. Wilson, Prof. B. J. Wiley
Department of Chemistry
Duke University
124 Science Drive, Box 90354, Durham,
North Carolina 27708, United States
E-mail: benjamin.wiley@duke.edu

Dr. Y.-C. Ha
Korea Electrotechnology Research Institute
Changwon 642–120, Republic of Korea



DOI: 10.1002/sml.201303005

diameter almost constant.^[5b] Markovich and coworkers demonstrated gold nanoparticles can be used to catalyze the growth of Au-Ag NWs with controlled diameters between 2 and 16 nm by changing the concentration of the seeds.^[5c] He *et al.* were able to grow vertically aligned Au NWs on a Si/SiO₂ substrate from the substrate-bound seeds.^[5d] However, a seeded approach has yet to be applied to the synthesis of Cu nanowires.

The fact that Cu is only 6% less conductive than the most conductive element, Ag, and yet is 1000 times more abundant, makes it a particularly attractive element from which to grow nanowires for a diverse range of applications that require high electrical conductivity. Several copper nanowire syntheses have been published, but there are two general approaches that are in use by multiple labs. One approach is to reduce CuCl₂ at ~175 °C in water under pressure for 10–48 hours in the presence of octadecylamine (or oleylamine, or hexadecylamine).^[6] A modification to this synthesis is the introduction of glucose as a reducing agent to decrease the reaction temperature to ~100 °C, and the reaction time to <6 hours.^[7] Attractive features of the alkylamine-mediated synthesis include the fact that the solvent is principally water, and that it can produce nanowires that are quite thin (as low as ~20 nm) and long (>100 μm). Such high-aspect ratio nanowires are desirable due to their superior performance in transparent conducting films.^[6b,8]

A second approach is the reduction of Cu(II) ions with hydrazine (N₂H₄) at <80 °C for <1 hr in an aqueous alkaline solution with EDA as a capping agent.^[1,8b] The fact that the EDA-mediated synthesis is several times faster than the alkylamine-mediated synthesis, and can be performed at ambient pressure (which greatly simplifies the taking of samples from the reaction), makes it more attractive for commercial production and mechanistic studies. This paper focuses on the EDA-mediated approach in an attempt to better understand the processes that govern the formation of copper nanowires in this reaction, and thus obtain nanowire aspect ratios comparable to the alkylamine-mediated synthesis. For example, it is not clear why seed particles form in the reaction. It is also not clear what roles EDA plays in the formation of copper nanowires.^[1,8b,9]

In this work, we use a combination of dark field optical microscopy (DFOM), SEM, TEM, EDS, XRD, and UV-Vis spectroscopy to further clarify the processes by which copper nanowires spontaneously form in solution. This study has identified Cu₂O particles as an important intermediate during the early stages of the reaction. We show that EDA prevents the growth of these Cu₂O particles into larger octahedra, instead causing them to aggregate and form the copper seeds from which nanowires subsequently grow. We use this new mechanistic information to develop the first seed-mediated synthesis of copper nanowires.^[5a,10] The introduction of Cu₂O octahedra as seeds to a copper nanowire synthesis improves the yield of nanowires and improves control over their dimensions. We used this synthesis to produce nanowires with different lengths, and demonstrate the effect of nanowire aspect ratio on the optical transparency and electrical conductivity of a copper nanowire network.

2. Results and Discussion

2.1. The Stages of a Copper Nanowire Reaction

The synthesis of copper nanowires described here is a modified version of a procedure described previously.^[1,9a] **Figure 1** illustrates the color changes of the reaction over time (A-C), along with DFOM and SEM images of the corresponding nanostructures suspended in the solution (D-F). The initial reaction mixture of 1 mL of 0.1 M Cu(NO₃)₂, 20 mL of 15 M NaOH, and 0.15 mL (2.25 mmol) of EDA (Figure 1A) has a deep blue color. UV-Vis absorbance spectra indicate the deep blue color is due to the formation of a [Cu(OH)₄]²⁻ complex (Figure S-1, Supporting Information).^[11] Although the formation constant of [Cu(EDA)₂]²⁺ ($K_f = 10^{20}$) is four orders of magnitude higher than that of [Cu(OH)₄]²⁻ ($K_f = 10^{16}$),^[9b] the absorbance peak of a solution containing the Cu(NO₃)₂ and NaOH did not change after the addition of EDA (Figure S-1). Conversely, a Cu(II)-EDA complex (1 mL of 0.1 M of Cu(NO₃)₂ and 0.15 mL of EDA) solution prepared at neutral pH turned blue after addition of 15 M NaOH. The formation of the [Cu(OH)₄]²⁻ complex is more favorable due to the high concentration of OH⁻ anions in solution.

This initial blue mixture was preheated at 50 °C with stirring for 5 min. N₂H₄ was then added, stirring stopped, and the flask was sealed with a stopper. The addition of N₂H₄ quickly turned the solution into a white, translucent suspension due to the bubbles of N₂ gas produced by the oxidation of N₂H₄ as it reduces [Cu(OH)₄]²⁻ to a colorless Cu(I) species. Thermodynamic calculations indicate this Cu(I) species is almost certainly [Cu(OH)₂]⁻ because this is the most thermodynamically stable Cu(I) species at a pH greater than 10 across a wide range of temperatures (25–300 °C).^[12] The bubbles dissipated and the solution turned clear (Figure 1B) after 10 min. SEM and DFOM images of a sample from the reaction during this clear stage revealed the presence of blue spherical particles, 70 ± 8 nm in diameter (Figure 1D). After an additional 40 min, the reaction remained clear, but the particles grew to form salmon-colored aggregates with diameters of 200–500 nm (Figure 1E). Nanowires with a diameter of ~45 nm grew out of the agglomerates by 60 min (Figure 1F), and the solution became dark red in color (Figure 1C).

The blue particles formed during the clear stage of the reaction were further characterized with TEM, XRD and EDS. Bright field TEM shows the presence of small particles with a size distribution of 69 ± 6 nm (**Figure 2A**), which agrees well with the SEM measurements. The XRD peaks centered at 29.6, 36.5, 42.4, 52.6, 61.6, and 73.7° corresponded to the {110}, {111}, {200}, {211}, {220}, and {311} planes of cubic Cu₂O, respectively (Figure 2B). EDS mapping also verified that the particles are composed of Cu and O (Figure 2C, D & E). Based on the TEM, XRD and EDS analyses, we were able to conclude that the particles are Cu₂O.

2.2. EDA Suppresses the Formation of Cu₂O Octahedra

If the amount of EDA in the Cu NW reaction is less than 0.60 mmol, rather than forming copper nanowires in 1 hr,

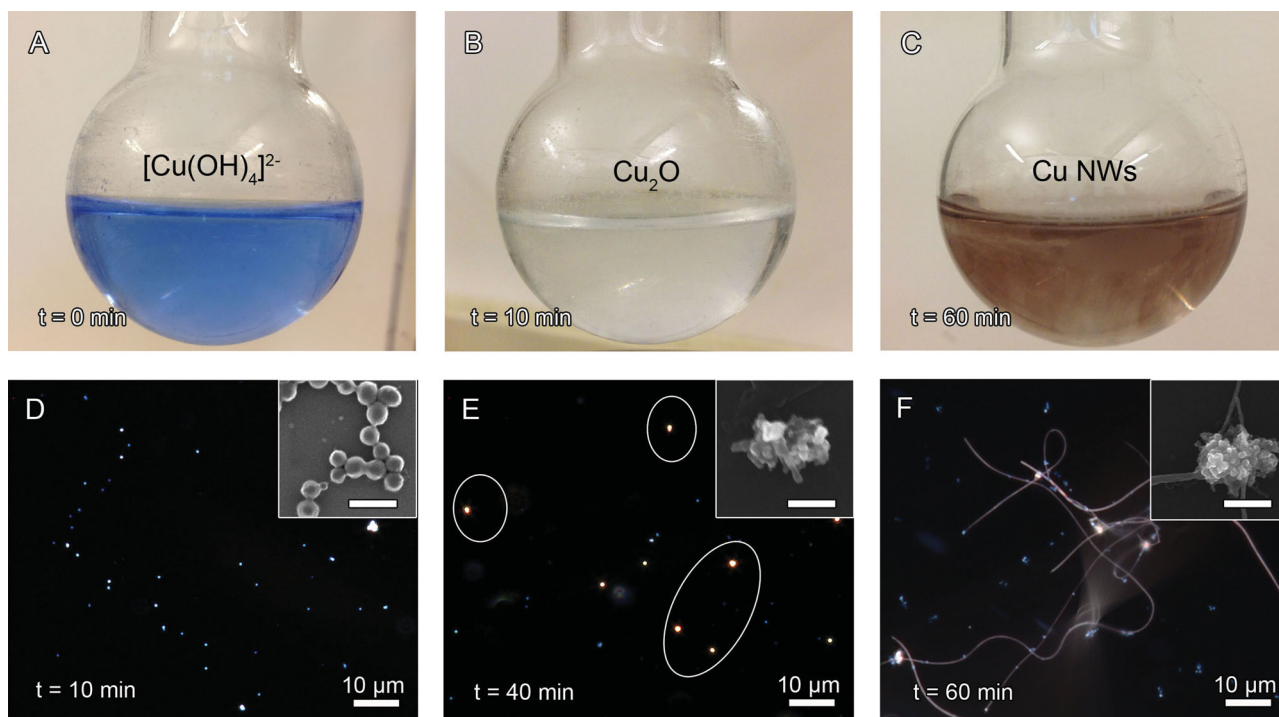


Figure 1. Stages of a copper nanowire reaction. A) The initial mixture of Cu(NO₃)₂, NaOH, and EDA is blue due to the formation of [Cu(OH)₄]²⁻. B) The solution becomes clear 10 min after addition of N₂H₄, and C) dark red after 60 min. DFOM images and corresponding SEM images (insets) of D) Cu₂O particles at 10 min, E) Cu agglomerates at 40 min, highlighted in circles, and F) Cu NWs at 60 min. Scale bars in insets are 200 nm.

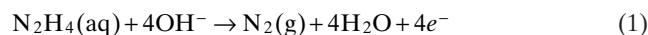
octahedra of Cu₂O form in <10 min (**Figure 3**). With no EDA, octahedra with an edge length of 230 nm were produced in 5 min (Figure 3A). As the EDA concentration was increased to 0.075, 0.15, 0.45 and 0.60 mmol, the octahedron edge length increased to 550, 865, 1680 and 3430 nm, respectively (Figure 3B, C, D & E). Note that the sides of the octahedra appear more concave with increasing EDA concentration (Figure 3D & E).

We hypothesize that the reason the particles grow larger with increasing EDA concentration is that EDA suppresses the nucleation of Cu₂O nanostructures. With no EDA, nucleation and growth of Cu₂O octahedra is very rapid (<2 min), resulting in a high concentration of Cu₂O precipitate (>60% Cu converted to Cu₂O at 2 min, see Figure 3F), and many small octahedra (230 nm). Further reduction of Cu₂O results in the formation of Cu particles with irregular shapes rather than copper nanowires (Figure S-2). At 0.15 mmol of EDA, the nucleation of the octahedra is suppressed, resulting in a lower concentration of Cu₂O precipitate (~10% conversion at 2 min and 55% at 5 min). The Cu₂O octahedra grew larger, albeit more slowly, at higher EDA concentrations because there were fewer nuclei to take up the Cu₂O precipitate. At the concentration of EDA (2.25 mmol) used for the production of Cu NWs, the Cu₂O particles that form at 10 min are amorphous in shape and small (70 nm, Figure 1E) compared to the concave octahedra (3430 nm, Figure 3E) that form at the same time when the concentration of EDA is lower (0.60 mmol). The more amorphous shape, smaller size, and lower concentration (~4% conversion) of Cu₂O precipitate at 10 min at the EDA concentration used for growing Cu NWs suggests that EDA suppresses the nucleation and growth of

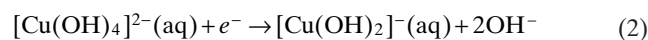
Cu₂O particles. Since copper nanowires do not form from the reduction of a Cu₂O precipitate (Figure S-2), this role of EDA in suppressing Cu₂O precipitation is critical to the formation of copper nanowires in solution.

2.3. A Revised Copper Nanowire Growth Mechanism

Scheme 1 illustrates a revised understanding of the copper nanowire growth mechanism that accounts for the role of Cu₂O seeds and EDA in copper nanowire growth. After the addition of hydrazine, the blue [Cu(OH)₄]²⁻ solution turns a translucent white after a few seconds due to the decomposition of hydrazine to N₂ gas via reaction Equation (1):



This first hydrazine oxidation reaction is coupled to the reduction of [Cu(OH)₄]²⁻ ions to [Cu(OH)₂]⁻ via Equation (2):



Some of the [Cu(OH)₂]⁻ complex then loses a water molecule and nucleates as Cu₂O particles:



Thus, the net reaction for Cu₂O nucleation is:

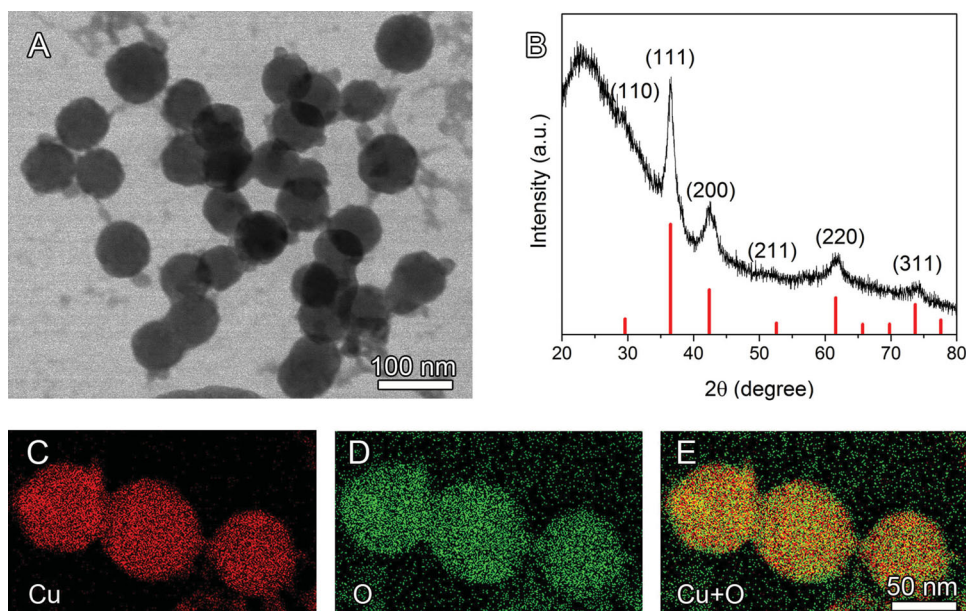
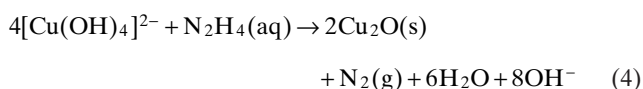
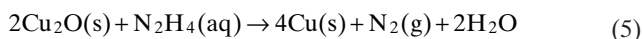


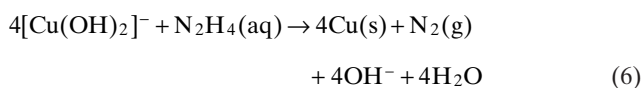
Figure 2. Characterization of Cu_2O particles by (A) bright field TEM, (B) powder XRD and (C-E) EDS mapping. All samples were extracted from the clear solution at 10 min. The broad XRD peak at 25° is from the glass substrate. The XRD pattern shown in red is the standard for Cu_2O (JCPDS #05-0667).



At low EDA concentrations (< 0.60 mmol), Equation (4) proceeds until the initial copper precursor is converted to Cu_2O octahedra. Cu_2O are eventually converted to Cu particles with irregular shapes via Equation (5):



If the EDA amount is > 2.25 mmol, a relatively small amount of Cu_2O nanoparticles form and are reduced to form metallic Cu aggregates via Equation (5). These Cu aggregates can then serve as seeds that sprout nanowires via reduction of ionic copper precursor:



We have previously shown that the copper nanowires that grow from the irregular polycrystalline Cu seeds have a five-fold twinned crystal structure.^[3c] Unlike the case of Ag nanowires, the Cu nanowires in this reaction do not grow from individually dispersed, pentagonally twinned decahedra.^[7b,13] Instead, the copper nanowires grow from irregularly shaped, polycrystalline copper seeds 200 to 500 nm in diameter, with secondary particles 40 nm in diameter (insets in Figure 1E and 1F) protruding from their surface. It seems likely that some of these secondary particles have a pentagonally twinned structure, and thus serve as sites for growth of pentagonally twinned copper nanowires. Indeed, a Cu nanorod with a clear twin boundary extending

along its length and into a secondary particle on a Cu seed can be observed by TEM imaging of a sample from a reaction at $t = 40$ min (Figure S-3). Such twin boundaries have previously been indicative of a pentagonally twinned crystal structure.^[7b,13a]

2.4. Planting Cu_2O Seeds to Control the Growth of Cu Nanowires

Using the new mechanistic understanding of the copper nanowire growth process, we can effectively separate the nucleation and nanowire growth steps by introducing Cu_2O seed particles to the reaction, and thereby improve the control over the dimensions of nanowires. A seed solution of Cu_2O octahedra was prepared by reacting an aqueous mixture of $\text{Cu}(\text{NO}_3)_2$, NaOH, and N_2H_4 for 2 min at 50°C (Figure 4A). The seed solution was then transferred to a growth solution consisting of $\text{Cu}(\text{NO}_3)_2$, NaOH, and EDA, followed by addition of N_2H_4 under fast stirring. Copper nanowires started to grow out of the added seed particles during the first several minutes of the reaction, and the reaction was complete in about one third of the time (15–20 min) required for the one-pot method. In addition, atomic absorption spectroscopy (AAS) measurements indicate the seeded synthesis produced a higher yield of nanowires (55–60%) compared to the one-pot method (~12%). SEM images of the resulting wires in Figure 4B & C show that the agglomerate particles at the interface of the Cu_2O octahedra and Cu NWs were similar in size and morphology to the ones previously observed in the one-pot method. The Cu_2O seeds remained intact as the copper nanowires grew, resulting in a Cu_2O -Cu heterostructure. The fact that the Cu_2O seed remained after nanowire growth is further confirmed by the coexistence of Cu and Cu_2O peaks in the XRD of the Cu_2O -Cu

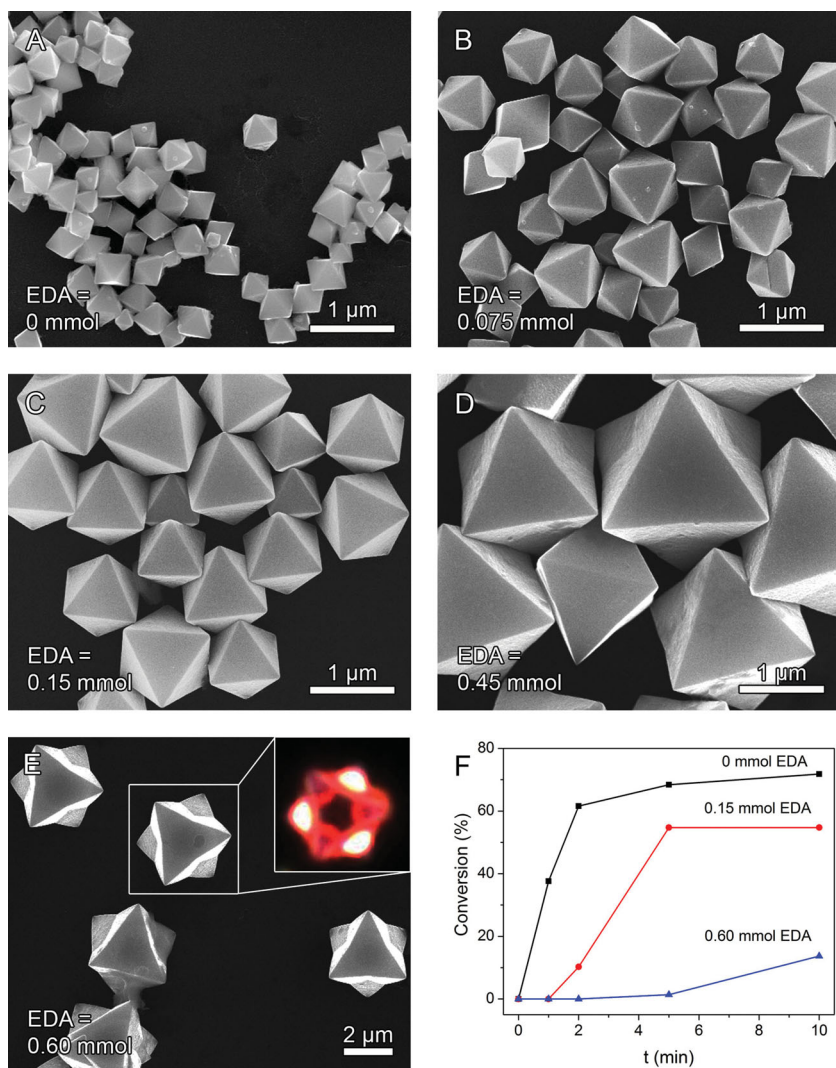


Figure 3. Size and morphological change of Cu₂O octahedra as a function of EDA concentration. The SEM images show Cu₂O octahedra (A–C), and concave octahedra (D,E). The inset in (E) is a DFOM image of an octahedron. (F) Conversion rate of copper precursor to Cu₂O particles in the presence of different concentrations of EDA.

heterostructures (Figure 4D). The presence of Cu₂O in the heterostructure was also verified by etching the oxide away using glacial acetic acid, leaving behind only metallic copper (Figure S-4).

A plot of nanowire length and diameter as a function of the ratio of seed to growth solution is shown in **Figure 5A**. By varying the concentration of the seeds to the growth solution, the length of the nanowires could be controllably varied from 18 to 51 μm, while maintaining the nanowire diameter at ~40 nm. Lower ratios of seed solution to growth solution resulted in longer nanowires with higher aspect ratios. Histograms of nanowire length and width are given in Figure S-5.

2.5. Transparent conducting films made of Cu nanowires with different aspect ratios

To fabricate transparent conducting electrodes, we transferred the nanowires from the original aqueous storage

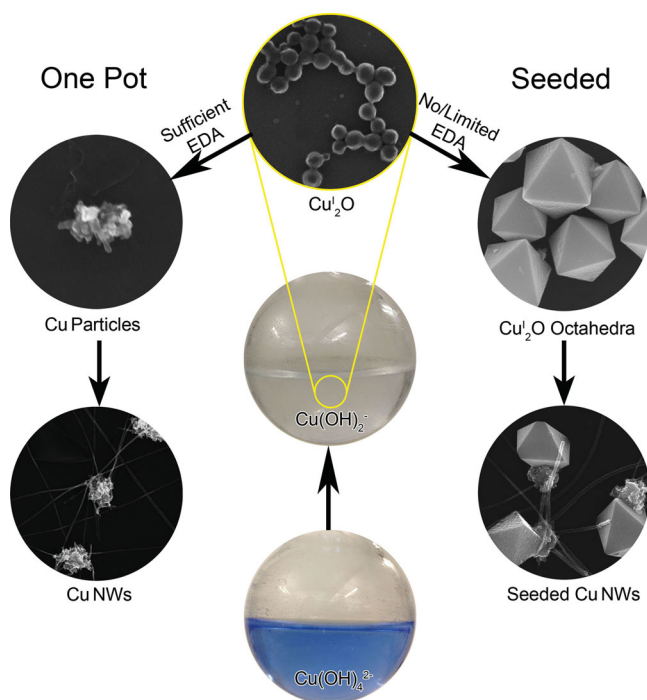
solution into an ink solution.^[3c,8b] A small volume of the nanowire ink suspension was coated with a Meyer rod onto a glass substrate, and allowed to dry in air. The resulting random network of copper nanowires made a film that was uniform over the area of the substrate without observable aggregation. The nanowire electrode was initially non-conductive due to the presence of nitrocellulose and native copper oxide on the surface of the nanowires. Plasma treatment of the nanowire network using forming gas and subsequent annealing under H₂ gas at 225–250 °C for 30 min resulted in a dramatic drop of the sheet resistance. The decrease in sheet resistance was attributed to the decomposition of nitrocellulose and the reduction of copper oxide to metallic copper, which allowed the copper nanowires to make contact and fuse together. The specular transmittance and sheet resistance of the copper nanowire networks were measured using a UV-Vis spectrophotometer and a four-point probe.

The specular transmittance versus the sheet resistance of the copper nanowire network with three different aspect ratios is shown in Figure 5B, along with previous literature results. The nanowire electrodes made of copper nanowires with higher aspect ratios led to better performance in terms of optical transparency and sheet resistance. For example, at a sheet resistance of 150 Ω sq⁻¹, the transmittance increases from 91.9% to 95.4% as the aspect ratio of the nanowires increases from 380 to 1130. This finding is consistent with previous reports that show higher aspect ratio nanowires enable a film to

achieve a lower sheet resistance at a given area coverage of nanowires due to the greater probability of higher aspect ratio nanowires to make contact with their neighbors.^[4,8a] The performance of films of the highest aspect ratio copper nanowires is comparable to the best reported results from previous solution-phase syntheses.^[1,6b,8b,c,16]

3. Conclusion

We have shown that the reduction of [Cu(OH)₄]²⁻ to [Cu(OH)₂]⁻ in the early stages of the EDA-mediated copper nanowire synthesis leads to the precipitation of Cu₂O nanoparticles, which in turn aggregate and are reduced to form the copper seeds from which nanowires sprout and grow. Removal of EDA from the copper nanowire synthesis leads to the rapid formation of Cu₂O octahedra. These Cu₂O octahedra can be added as seeds to a copper nanowire synthesis to control the number of nanowires, and thus the length



Scheme 1. Proposed reaction pathway of EDA-dependent copper reduction.

of nanowires, that form in a reaction. We produced nanowires with different lengths to demonstrate the relationship between the aspect ratio of copper nanowires and their performance in transparent conducting films. The improved control of copper nanowire dimensions enabled by this seeded approach will lead to a better understanding of the structure-property relationship of copper nanowires in a variety of applications.

4. Experimental Section

Synthesis of Copper Nanowires through the One-Pot Method: $\text{Cu}(\text{NO}_3)_2$ (Sigma-Aldrich, 0.1 M, 1 mL), NaOH (Acros Organics, 15 M, 20 mL) and EDA (Sigma-Aldrich, 150 μL) were mixed in a 50 mL round bottom flask with a glass stopper and heated to 50 °C at a stirring rate of 700 rpm. N_2H_4 (Sigma-Aldrich, 35 wt%, 25 μL) was quickly injected into the above solution after stirring for 5 min. Upon addition of N_2H_4 , the mixture initially turned white and cloudy, and changed to a clear and colorless solution within the first 2 min. The solution remained clear till $t = \sim 60$ min when a dark red color slowly appeared throughout the entire solution. An aqueous solution (~ 15 mL) containing 3% PVP (polyvinylpyrrolidone, Sigma-Aldrich, MW = 10 K) and 1% DEHA (diethylhydroxylamine, Acros Organics) was added to the growth solution to collect the nanowires. The mixture was then

transferred to a separation funnel and vigorously shaken until a white clump of PVP and nanowires floated to the surface. The bottom solution was drained and fresh PVP/DEHA solution was added to re-disperse the nanowires. Cu NWs were then purified with 1% DEHA solution for further characterization by three cycles of centrifugation (10 min at 2000 rpm) and decantation. The typical SEM (FEI XL30 SEM-FEG) samples were prepared by drying the purified nanowire solution on a silicon wafer under nitrogen flow. The purified nanowire solution was also dried on a Cu grid for TEM (FEI Tecnai G² Twin) and on a glass slide for XRD (Panalytical X'Pert PRO MRD) under nitrogen. During the course of the reaction, small aliquots of the reaction solution were drawn and imaged with a dark field optical microscope (Olympus BX51 fitted with a SC30 CMOS camera). The SEM samples in Figure 1 were prepared by dipping a small piece of plasma cleaned silicon wafer into the reaction solution at a given time point for 15 seconds. The wafer was rinsed with 3% DEHA solution and dried under nitrogen protection.

Seeded Synthesis of Copper Nanowires: Seed solution was prepared by adding N_2H_4 (35%, 25 μL) into a preheated mixture (50 °C, stirred at 700 rpm) of $\text{Cu}(\text{NO}_3)_2$ (0.1 M, 1 mL), NaOH (15 M, 20 mL). After stirring for 2 min, 5 mL, 2 mL, or 1 mL of seed solution was transferred to a preheated growth solution (50 °C, stirred at 700 rpm) containing $\text{Cu}(\text{NO}_3)_2$ (0.1 M, 1 mL), NaOH (15 M, 20 mL) and EDA (150 μL , 2.25 mmol), to produce nanowires with an aspect ratio of 380, 720, and 1130, respectively. N_2H_4 (35 wt%, 25 μL) was then added, the stirring was stopped after 2 min, and the mixture slowly changed from orange to deep red over the next 20 min. Nanowires were washed and prepared for characterization in the same manner as with the one-pot synthesis.

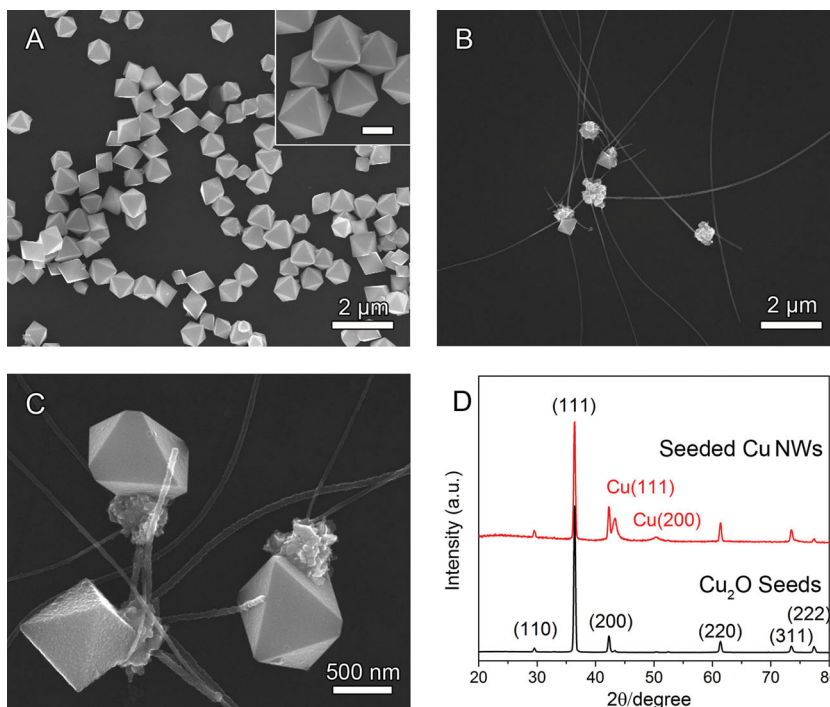


Figure 4. Seeded growth of copper nanowires through the addition of Cu_2O octahedral particles. SEM images of (A) Cu_2O octahedral seeds and (B & C) Cu_2O octahedra – Cu NWs heterostructures. Inset scale bar is 500 nm. (D) The XRD patterns of Cu_2O seeds (black curve) and Cu_2O -seeded Cu NWs (red).

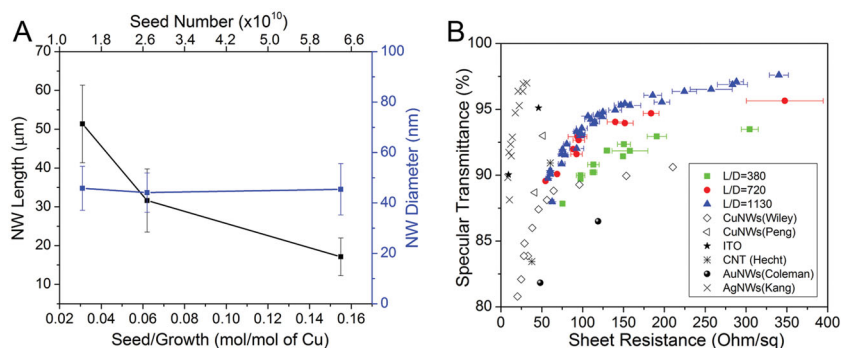


Figure 5. (A) The effect of the seed/growth ratio on the length and diameter of the nanowires; (B) Plot of specular transmittance (%) at 550 nm wavelength versus sheet resistance of copper nanowire electrodes with three different aspect ratios. Also shown for comparison are data representing the state of the art transparent conductive networks of CuNWs (Wiley,^[8b] Peng),^[6b] Ag NWs (Kang),^[8d] Au NWs (Coleman),^[14] and carbon nanotubes (Hecht).^[15]

Synthesis of Cu₂O Octahedral Particles with Different Sizes: A mixture of Cu(NO₃)₂ (0.1 M, 1 mL), NaOH (15 M, 20 mL) and a certain amount of EDA was preheated with stirring at 700 rpm for 5 min at 50 °C. 0, 0.075, 0.15, 0.45, and 0.60 mmol of EDA was used to prepare octahedra with edge lengths of 230, 550, 865, 1680, 3430 nm, respectively. After N₂H₄ (35%, 25 μL) was added, the solution turned orange and Cu₂O octahedra formed. The Cu₂O particles were collected using the PVP/DEHA solution and purified with 1% DEHA solution for further characterization with SEM and XRD. To determine the conversion rate of ionic copper to Cu₂O, the Cu₂O particles were filtered from the solution at different time points. The collected particles were then dissolved in concentrated nitric acid (1 mL) and diluted to a set volume. The concentration of copper was analyzed using an atomic absorption spectrometer (Perkin Elmer 3100).

Preparation of Transparent Conducting Electrodes: Transparent electrodes were made in a manner similar to that which was previously reported.^[8b] The Cu NW solution in 1% DEHA was transferred into a 1.5 mL centrifuge tube and centrifuged at ~2000 rpm for 1 min. The Cu NWs were washed 3 times using a solution of 3% DEHA containing no PVP to ensure PVP was removed. After the PVP was removed, the Cu NWs were washed with ethanol (Koptec) to remove the majority of the water and then washed once more with the ink formulation. The ink formulation was made by dissolving nitrocellulose (Scientific Polymer, 0.06 g) in acetone (BDH, 2.94 g) and then adding ethanol (3 g), ethyl acetate (Sigma-Aldrich, 0.5 g), pentyl acetate (Sigma-Aldrich, 1 g), isopropanol (Sigma-Aldrich, 1 g), and toluene (Sigma-Aldrich, 1.7 g). After the Cu NWs (~3 mg) were washed with the ink formulation, additional ink formulation (0.3 mL) was added to the Cu NWs, and this suspension was vortexed. To prepare a transparent nanowire electrode, glass microscope slides were placed onto a clipboard to hold them down while the nanowire ink (50 μL) was pipetted in a line at the top of the slide. A Meyer rod (Gardco #13, 33.3 μm wet film thickness) was then quickly (<1 second) pulled down over the nanowire ink by hand, spreading it across the glass into a thin, uniform film. Different densities of nanowires on the surface of the substrate were obtained by varying the concentration of the nanowires in the ink. The film was dry after approximately 60 seconds. To remove organic material from the nanowire network, the films were cleaned in a plasma cleaner (Harrick

Plasma PDC-001) for 10 minutes in an atmosphere of 95% nitrogen and 5% hydrogen at a pressure of 600–700 mTorr. The nanowire films were then heated at 250 °C in a tube furnace for 30 minutes under a constant flow of hydrogen (350 mL min⁻¹) to anneal the wires together and decrease the sheet resistance. The transmittance and sheet resistance of each nanowire film was measured using a UV-Vis-NIR spectrophotometer (Cary 6000i) and a four-point probe (Signatone SP4–50045TBS). Each data point in Figure 5B is the average of 5 measurements. Each data point also shows error bars that indicate one standard deviation.

Supporting Information

Supporting Information is available from the Wiley Online Library or from the author.

Acknowledgements

This work was supported in part by the National Science Foundation's (NSF's) Research Triangle MRSEC (DMR-1121107), an NSF CAREER award (DMR-1253534), and NSF grant no. ECCS-1344745.

- [1] A. R. Rathmell, S. M. Bergin, Y.-L. Hua, Z.-Y. Li, B. J. Wiley, *Adv. Mater.* **2010**, *22*, 3558.
- [2] a) C. D. Keating, M. J. Natan, *Adv. Mater.* **2003**, *15*, 451; b) A. V. Akimov, A. Mukherjee, C. L. Yu, D. E. Chang, A. S. Zibrov, P. R. Hemmer, H. Park, M. D. Lukin, *Nature* **2007**, *450*, 402; c) S. Lal, S. Link, N. J. Halas, *Nat. Photon* **2007**, *1*, 641; d) A. Tao, F. Kim, C. Hess, J. Goldberger, R. He, Y. Sun, Y. Xia, P. Yang, *Nano Lett.* **2003**, *3*, 1229; e) D. P. Burt, N. R. Wilson, J. M. R. Weaver, P. S. Dobson, J. V. Macpherson, *Nano Lett.* **2005**, *5*, 639; f) T. Thurn-Albrecht, J. Schotter, G. A. Kästle, N. Emley, T. Shibauchi, L. Krusin-Elbaum, K. Guarini, C. T. Black, M. T. Tuominen, T. P. Russell, *Science* **2000**, *290*, 2126; g) L. Piraux, J. M. George, J. F. Despres, C. Leroy, E. Ferain, R. Legras, K. Ounadjela, A. Fert, *Appl. Phys. Lett.* **1994**, *65*, 2484.
- [3] a) J.-Y. Lee, S. T. Connor, Y. Cui, P. Peumans, *Nano Lett.* **2008**, *8*, 689; b) S. De, T. M. Higgins, P. E. Lyons, E. M. Doherty, P. N. Nirmalraj, W. J. Blau, J. J. Boland, J. N. Coleman, *ACS Nano* **2009**, *3*, 1767; c) A. R. Rathmell, M. Nguyen, M. Chi, B. J. Wiley, *Nano Lett.* **2012**, *12*, 3193; d) J. van de Groep, P. Spinelli, A. Polman, *Nano Lett.* **2012**, *12*, 3138; e) R. Chen, S. R. Das, C. Jeong, M. R. Khan, D. B. Janes, M. A. Alam, *Adv. Funct. Mater.* **2013**, *23*, 5150.
- [4] S. M. Bergin, Y.-H. Chen, A. R. Rathmell, P. Charbonneau, Z.-Y. Li, B. J. Wiley, *Nanoscale* **2012**, *4*, 1996.
- [5] a) N. R. Jana, L. Gearheart, C. J. Murphy, *Chem. Comm.* **2001**, 617; b) J. Lee, P. Lee, H. Lee, D. Lee, S. S. Lee, S. H. Ko, *Nanoscale* **2012**, *4*, 6408; c) D. Azulai, E. Cohen, G. Markovich, *Nano Lett.* **2012**, *12*, 5552; d) J. He, Y. Wang, Y. Feng, X. Qi, Z. Zeng, Q. Liu, W. S. Teo, C. L. Gan, H. Zhang, H. Chen, *ACS Nano* **2013**, *7*, 2733.

- [6] a) Y. Shi, H. Li, L. Chen, X. Huang, *Sci. Technol. Adv. Mater.* **2005**, *6*, 761; b) H. Guo, N. Lin, Y. Chen, Z. Wang, Q. Xie, T. Zheng, N. Gao, S. Li, J. Kang, D. Cai, D.-L. Peng, *Sci. Rep.* **2013**, *3*, 2323.
- [7] a) M. Mohl, P. Puszta, A. Kukovec, Z. Konya, J. Kukkola, K. Kordas, R. Vajtai, P. M. Ajayan, *Langmuir* **2010**, *26*, 16496; b) M. Jin, G. He, H. Zhang, J. Zeng, Z. Xie, Y. Xia, *Angew. Chem. Int. Ed.* **2011**, *50*, 10560.
- [8] a) R. M. Mutiso, M. C. Sherrott, A. R. Rathmell, B. J. Wiley, K. I. Winey, *ACS Nano* **2013**, *7*, 7654; b) A. R. Rathmell, B. J. Wiley, *Adv. Mater.* **2011**, *23*, 4798; c) D. Zhang, R. Wang, M. Wen, D. Weng, X. Cui, J. Sun, H. Li, Y. Lu, *J. Am. Chem. Soc.* **2012**, *134*, 14283; d) M. Song, D. S. You, K. Lim, S. Park, S. Jung, C. S. Kim, D.-H. Kim, D.-G. Kim, J.-K. Kim, J. Park, Y.-C. Kang, J. Heo, S.-H. Jin, J. H. Park, J.-W. Kang, *Adv. Funct. Mater.* **2013**, *23*, 4177.
- [9] a) Y. Chang, M. L. Lye, H. C. Zeng, *Langmuir* **2005**, *21*, 3746; b) F. Meng, S. Jin, *Nano Lett.* **2012**, *12*, 234; c) A. P. Periasamy, J. Liu, H.-M. Lin, H.-T. Chang, *J. Mater. Chem. A* **2013**, *1*, 5973.
- [10] a) N. R. Jana, L. Gearheart, C. J. Murphy, *J. Phys. Chem. B* **2001**, *105*, 4065; b) Y. Sun, B. Gates, B. Mayers, Y. Xia, *Nano Lett.* **2002**, *2*, 165; c) X. Xia, J. Zeng, L. K. Oetjen, Q. Li, Y. Xia, *J. Am. Chem. Soc.* **2011**, *134*, 1793; d) S. E. Habas, H. Lee, V. Radmilovic, G. A. Somorjai, P. Yang, *Nat. Mater.* **2007**, *6*, 692; e) C. Xue, J. E. Millstone, S. Li, C. A. Mirkin, *Angew. Chem. Int. Ed.* **2007**, *46*, 8436; f) F.-R. Fan, D.-Y. Liu, Y.-F. Wu, S. Duan, Z.-X. Xie, Z.-Y. Jiang, Z.-Q. Tian, *J. Am. Chem. Soc.* **2008**, *130*, 6949; g) Y.-H. Chen, H.-H. Hung, M. H. Huang, *J. Am. Chem. Soc.* **2009**, *131*, 9114; h) J. Zeng, Y. Zheng, M. Rycenga, J. Tao, Z.-Y. Li, Q. Zhang, Y. Zhu, Y. Xia, *J. Am. Chem. Soc.* **2010**, *132*, 8552.
- [11] Y.-Y. H. Chao, D. R. Kearns, *J. Phys. Chem.* **1977**, *81*, 666.
- [12] B. Beverskog, I. Puigdomenech, *J. Electrochem. Soc.* **1997**, *144*, 3476–3483.
- [13] a) Y. Sun, B. Mayers, T. Herricks, Y. Xia, *Nano Lett.* **2003**, *3*, 955; b) B. Wiley, Y. Sun, Y. Xia, *Acc. Chem. Res.* **2007**, *40*, 1067.
- [14] P. E. Lyons, S. De, J. Elias, M. Schamel, L. Philippe, A. T. Bellew, J. J. Boland, J. N. Coleman, *J. Phys. Chem. Lett.* **2011**, *2*, 3058.
- [15] D. S. Hecht, A. M. Heintz, R. Lee, L. Hu, B. Moore, C. Cucksey, S. Risser, *Nanotechnology* **2011**, *22*, 075201.
- [16] I. N. Kholmanov, S. H. Domingues, H. Chou, X. Wang, C. Tan, J.-Y. Kim, H. Li, R. Piner, A. J. G. Zarbin, R. S. Ruoff, *ACS Nano* **2013**, *7*, 1811.

Received: September 16, 2013

Revised: November 28, 2013

Published online: